

RESEARCH

Open Access



Mathematical analysis and numerical simulation of two-component system with non-integer-order derivative in high dimensions

Kolade M Owolabi* and Abdon Atangana

*Correspondence:
mkowolax@yahoo.com
Institute for Groundwater Studies,
Faculty of Natural and Agricultural
Sciences, University of the Free
State, Bloemfontein, 9300, South
Africa

Abstract

In this paper, we propose efficient and reliable numerical methods to solve two notable non-integer-order partial differential equations. The proposed algorithm adapts the Fourier spectral method in space, coupled with the exponential integrator scheme in time. As an advantage over existing methods, our method yields a full diagonal representation of the non-integer fractional operator, with better accuracy over a finite difference scheme. We realize in this work that evolution equations formulated in the form of fractional-in-space reaction-diffusion systems can result in some amazing examples of pattern formation. Numerical experiments are performed in two and three space dimensions to justify the theoretical results. Simulation results revealed that pattern formation in a fractional medium is practically the same as in classical reaction-diffusion scenarios.

MSC: 34A34; 35A05; 35K57; 65L05; 65M06; 93C10

Keywords: Fourier spectral method; exponential integrator; fractional reaction-diffusion; nonlinear PDEs; numerical simulations; Turing instability

1 Introduction

Systems with non-integer order are commonly referred to as fractional differential equations. They are systems containing fractional integrals or fractional derivatives, which have received a lot of attention across disciplines such as biology, chemistry and physics. More importantly, they are mostly used in dynamical systems with chaotic and spatio-temporal dynamical behavior, quasi-chaotic dynamical systems, the dynamics of porous media or complex material and random walks with memory. The concepts of fractional differential equations, with fractional integral equations and fractional partial differential equations, have gained a wider application in diverse fields of applied science and engineering.

In some years back, the interest of some researchers was devoted to research on the equations involving the fractional differential equations applied to mechanics, physics, and other disciplines. For instance, the time-fractional reaction-diffusion equations have been studied by Podlubny [1], Podlubny *et al.* [2], Gorenflo *et al.* [3], Guo *et al.* [4], Gómex-

Aguilar *et al.* [5–8], Zhou [9], Ilic *et al.* [10] and Kilbas *et al.* [11] and the references therein, to mention a few. The interested reader is referred to the monographs and literature on fractional calculus.

However, recent years have been characterized by fast growing applications of fractional calculus to various scientific and engineering fields pertaining to anomalous diffusion, signal processing and control, constitutive modelling in viscoelasticity, image processing, fluid mechanics and findings on soft matter behavior, to mention a few. Unlike the integer-order ordinary or partial differential equations, fractional calculus is capable of providing a more detail, simple and accurate description of complex dynamical, mechanical, chemical and physical processes that feature historical dependence and space non-locality, which has induced the occurrences of a series of fractional differential equations.

However, the mathematical theory and the efficient numerical algorithms of fractional-order differential equations require further study. Most analytical solutions obtained for fractional differential problems are given in terms of special functions, which make numerical evaluation difficult and almost impossible. Until now, finite difference schemes and series approximation techniques such as the variational iteration method and the Adomian decomposition method remain the dominant numerical methods for the solution of fractional reaction-diffusion equations.

More importantly, little is now known about the systematic analyses on the issue of stability of numerical methods regarding fractional calculus, together with the solution techniques for high-dimensional fractional reaction-diffusion equations, most especially for nonlinear equations. The present paper introduces the Fourier spectral method as a better alternative to finite difference methods for solving fractional-in-space reaction-diffusion systems in one and high dimensions.

The remainder part of this paper is broken into sections. In Section 2, we introduce the general two-components partial differential equations formulated in both classical and fractional reaction-diffusion systems. We provide conditions for the emergence of Turing instability in the two scenarios. Section 3 deals with the basics of fractional derivatives and various methods of numerical approximations. Numerical experiments in high dimensions are presented with some notable examples taken from the literature in Section 4. Section 5 concludes the paper.

2 Model equation

In this section, we consider a two species scaled and nondimensionalized system in the form [12–14]

$$\left. \begin{aligned} \frac{\partial u(x,t)}{\partial t} &= D_u \Delta^2 u(x,t) + \mathcal{F}(u,v), \\ \frac{\partial v(x,t)}{\partial t} &= D_v \Delta^2 v(x,t) + \mathcal{G}(u,v), \end{aligned} \right\} \quad (2.1)$$

where $u(x,t), v(x,t)$ are used to describe the concentration of species at spatial position x and time t , due to the presence of diffusion, with respective diffusion coefficients $D_u > 0, D_v > 0$. The nonlinear functions describing the reaction kinetics are given by \mathcal{F} and \mathcal{G} . System (2.1) can be solved using any of the boundary conditions, namely Neumann (zero-flux), Dirichlet, periodic or Robin type on bounded domain $\Omega \subset \mathbf{R}^n$. The chemical species concentrations are specified at $t = 0, \forall x \in \Omega$.

In what follows, we shall examine some existing background theorems and definitions that are well established for the general two-component reaction-diffusion system (2.1)

subject to zero-flux boundary conditions $v(\frac{u}{v}) = 0$, on $\partial\Omega \times [0, T)$ with the initial function $u = u_0, v = v_0$ on $\Omega \times \{t = 0\}$, on smooth and bounded domain Ω , satisfying the conditions: (i) existence and uniqueness, (ii) existence for all times t , (iii) continuously dependency on the initial functions, (iv) for non-negative initial data, the solution is non-negative, and (v) the solution is bounded for all given bounded initial data.

Definition 2.1 (Sectorial operator [15]) Let operator A be linear in a Banach space, denoted \mathcal{B} , and assume A is dense and closely defined. If there exist $a, \omega \in (0, \pi), \mathcal{M} \geq 1$, such that

$$\rho(A) \supset \Sigma = \{ \lambda \in \mathbb{C} \mid \varphi \leq \arg(\lambda - a) \leq \pi, \lambda \neq a \}$$

and

$$\|R_\lambda(A)\| \leq \frac{\mathcal{M}}{|\lambda - a|} \quad \text{for all } \lambda \in \Sigma, \tag{2.2}$$

where A is defined as a sectorial operator.

Theorem 2.2 *If A is given as a sectorial operator, then $-A$ is the corresponding infinitesimal generator of an analytic semigroup, $G(t)$. If $\text{Re } \lambda > a, a \in \mathbb{R}$, whenever $\lambda \in \sigma(A)$ then, for any $t > 0$,*

$$\|G(t)\| \leq C \exp(-at), \quad \|AG(t)\| \leq \frac{C}{t} \exp(-at).$$

Hence,

$$\frac{d}{dt}G(t) = -AG(t), \quad t > 0.$$

Proof The reader is referred to Theorem 1.3.4 in [15]. □

Lemma 2.3 *If u and v are continuous from $[0, T]$ to $L^p(\Omega)$, then the integrals*

$$\begin{aligned} I_1(t) &= \int_0^t G_1(t - \tau) \mathcal{F}(\tau, u(\tau), v(\tau)) \, d\tau, \\ I_2(t) &= \int_0^t G_2(t - \tau) \mathcal{G}(\tau, u(\tau), v(\tau)) \, d\tau, \end{aligned}$$

exist, G_1 and G_2 are the respective analytical semigroup of the Laplacian operators $\mathcal{L} = -\Delta$ and $D(\mathcal{L})$, I_1 and I_2 are continuous on $[0, T)$ with $I_1(t), I_2(t) \in \mathcal{D}(\mathcal{L})$ and $I_1(t), I_2(t) \rightarrow 0^+$ in L^p for $t \rightarrow 0^+$.

Proof If the reaction-diffusion system (2.1) has a classical solution, then u and v satisfy

$$\left. \begin{aligned} u(t) &= G_1(t)u_0 + \int_0^t G_1(t - \tau) \mathcal{F}(\tau, u(\tau), v(\tau)) \, d\tau, \\ v(t) &= G_2(t)v_0 + \int_0^t G_2(t - \tau) \mathcal{G}(\tau, u(\tau), v(\tau)) \, d\tau. \end{aligned} \right\} \tag{2.3}$$

The continuity of u, v indicates continuity of $t \mapsto \mathcal{F}(u(t), v(t), t)$ and $t \mapsto \mathcal{G}(u(t), v(t), t)$, so that the linear problems $\partial_t U - \Delta U = \mathcal{F}(u(t), v(t), t)$ and $\partial_t V - D\Delta V = \mathcal{G}(u(t), v(t), t)$ and $U(0) = u_0, V(0) = v_0$ have a unique solution. For details of the proof, see Lemma 3.2.1 in [15]. □

Theorem 2.4 (Local existence [15, 16]) *Assume the following conditions.*

- (c1) $D > 0$;
- (c2) $u_0 \geq 0$ and $v_0 \geq 0$ are continuous on $\bar{\Omega}, u_0, v_0 \in C_{L^\infty}^0(\Omega)$;
- (c3) \mathcal{F} and \mathcal{G} are said to be continuously differentiable from $\mathbb{R}_+^2 \rightarrow \mathbb{R}$ with $\mathcal{F}(0, y, t) \geq 0$ and $\mathcal{G}(x, 0, t) \geq 0$ for all $x, y, t \geq 0$, a situation applicable when $(x, y) \mapsto \mathcal{F}(x, y)$ and $(x, y) \mapsto \mathcal{G}(x, y)$ are differentiable for $\inf_{\Omega} \underline{u} \leq x \leq \sup_{\Omega} \bar{u}, \inf_{\Omega} \underline{v} \leq y \leq \sup_{\Omega} \bar{v}$ by the mean value theorem;
- (c4) There exist $m > 0$ and a continuous function $F_c : \mathbb{R}_+^2 \rightarrow \mathbb{R}_+$ such that $\mathcal{F}(x, y, t), \mathcal{G}(x, y, t) \leq \exp(mt)F_c(x, y)$ for all $x, y, t \geq 0$;

are satisfied. Then there exists $T = T(u_0, v_0)$ such that the reaction-diffusion system (2.1) possesses a unique solution $(u, v) \in [C_{L^\infty}^0((0, T]; \mathcal{D}(\mathcal{H}^\alpha))]^2$ with $u(0) = u_0 \in C_{L^\infty}^0$ and $v(0) = v_0 \in C_{L^\infty}^0$. For $\alpha \geq 0$ we give the fractional powers of the Helmholtz operator $\mathcal{H} = -\Delta + I$, which we denote \mathcal{H} and $\mathcal{D}(\mathcal{H}^\alpha)$ as the domain of fractional powers of \mathcal{H} .

Proof It suffices to establish the corresponding result for (2.3). See a similar proof in [15], Theorem 3.3.1, which utilized Banach’s fixed point theorem for establishing the result. □

2.1 Classical two-components reaction-diffusion systems

A Turing instability (diffusion-driven instability) arises when a homogeneous steady state solution of the reaction system of the form (2.1) is linearly stable to some perturbations in the absence of the diffusion terms (D_u, D_v) but linearly unstable in the presence of diffusion to small spatial perturbations. A spatially uniform steady state of the system (2.1) is the state $(u^*, v^*) : \mathcal{F}(u^*, v^*) = \mathcal{G}(u^*, v^*) = 0$ in such a way that $u = u^*, v = v^*$ satisfies the boundary conditions. For instance, using a zero-flux boundary condition on a rectangular domain, for diffusion-driven instability to occur, the conditions

$$\left. \begin{aligned} \frac{\partial \mathcal{F}}{\partial u} + \frac{\partial \mathcal{G}}{\partial v} &< 0, \\ \frac{\partial \mathcal{F}}{\partial u} \frac{\partial \mathcal{G}}{\partial v} - \frac{\partial \mathcal{F}}{\partial v} + \frac{\partial \mathcal{G}}{\partial u} &> 0, \\ D_u \frac{\partial \mathcal{G}}{\partial v} + D_v \frac{\partial \mathcal{F}}{\partial u} &> 0, \\ D_u \frac{\partial \mathcal{G}}{\partial v} + D_v \frac{\partial \mathcal{F}}{\partial u} &> 2\sqrt{D_u D_v \left(\frac{\partial \mathcal{F}}{\partial u} \frac{\partial \mathcal{G}}{\partial v} - \frac{\partial \mathcal{F}}{\partial v} + \frac{\partial \mathcal{G}}{\partial u} \right)}, \end{aligned} \right\} \tag{2.4}$$

must be satisfied. We evaluate the partial derivatives of \mathcal{F} and \mathcal{G} at the stationary uniform state (u^*, v^*) , that is, the zeros of \mathcal{F} and \mathcal{G} . The linear stability for the time evolution of the perturbations

$$(\nabla u(x, t), \nabla v(x, t))$$

about the equilibrium steady state (u^*, v^*) in the standard two-components system are given by

$$\left. \begin{aligned} \frac{\partial \nabla u(x, t)}{\partial t} &= \Delta^2 \nabla u(x, t) + \lambda(a_{11} \nabla u + a_{12} \nabla v), \\ \frac{\partial \nabla v(x, t)}{\partial t} &= D \Delta^2 \nabla v(x, t) + \lambda(a_{21} \nabla v + a_{22} \nabla u), \end{aligned} \right\} \tag{2.5}$$

where $D = D_u/D_v$ denotes the diffusivity ratio, $\lambda > 0$ is a scaling variable which can be defined as the relative strength of the reaction kinetics or as the linear size of the spatial domain, and

$$a_{i,j} = \left(\frac{\partial \mathcal{F}_i}{\partial n_j}, \frac{\partial \mathcal{G}_i}{\partial n_j} \right).$$

Next, for simplicity, we adopt the Laplace transform technique in the case of anomalous diffusion to find the Turing conditions. On applying a temporal Laplace and spatial Fourier transform, we obtain

$$\begin{aligned} \widehat{\widetilde{u}}(k,r) &= \frac{(r + Dk^2 - \lambda a_{22})\widetilde{\Delta u}(k, t = 0) + \lambda a_{12}\widetilde{\Delta v}(k, t = 0)}{(r + k^2 - \lambda a_{11})(r + Dk^2 - \lambda a_{22}) - \lambda^2 a_{12}a_{21}}, \\ \widehat{\widetilde{v}}(k,r) &= \frac{(r + k^2 - \lambda a_{11})\widetilde{\Delta v}(k, t = 0) + \lambda_{21}\widetilde{\Delta u}(k, t = 0)}{(r + k^2 - \lambda a_{11})(r + Dk^2 - \lambda a_{22}) - \lambda^2 a_{12}a_{21}}, \end{aligned}$$

where k, r are the Fourier and Laplace transform variables, the tilde and hat symbols denote, respectively, the Fourier and Laplace transformed variables. By finding the inverse of the Laplace transforms, we obtain the perturbations temporal growth

$$(r + k^2 - \lambda a_{11})(r + Dk^2 - \lambda a_{22}) - \lambda^2 a_{12}a_{21} = (r - s_1(k))(r - s_2(k)) \tag{2.6}$$

after factorizing the denominator and using partial fractions. If the roots in (2.6) are found to be distinct, the inverted canonical expression can be written in the form

$$\widehat{\widetilde{z}}(k,r) = \sum_{j=1}^2 \frac{\beta - j(k)}{r - s_j(k)},$$

with the corresponding inverse Laplace transform as

$$\widehat{\widetilde{z}}(k,t) = \sum_{j=1}^2 \beta - j(k)e^{s_j(k)t}.$$

For any of the roots to be positive (that is, having a real component greater than zero), the homogeneous steady state becomes linearly unstable, but linearly stable if otherwise. In what follows, we quickly summarized the conditions for a Turing (diffusion-driven) instability as (i) $\Re(s_1(k = 0)) < 0, \Re(s_2(k = 0)) < 0$, and (ii) $\Re(s_1(k > 0)) > 0, \Re(s_2(k > 0)) > 0$, with s_q defined as the zeros of the quadratic equation

$$\widehat{p}(s) = (s + k^2 - \lambda a_{11})(s + Dk^2 - \lambda a_{22}) - \lambda^2 a_{12}a_{21}.$$

It follows from equation (2.6) that, with the conditions $a_{11} + a_{22} < 0$ and $a_{11}a_{22}a_{12}a_{21} > 0$, condition (i) is consistent, but not so for (ii) in conjunction with (i) if $D = 1$. Conditions (i) and (ii) cannot be attained simultaneously if $D \leq 1$. In the physical sense, it implies that the necessary condition for a diffusion-driven (Turing) instability to give rise to pattern formation in a two-component system is that one of the species must diffuse faster than the other [12].

2.2 General two-components fractional reaction-diffusion systems

So far, we have examined the classical reaction-diffusion system. Here, we now consider the fraction reaction-diffusion system, a special case of (2.1) written in the general form

$$\left. \begin{aligned} \frac{\partial u(x,t)}{\partial t} &= \Delta^\alpha u(x,t) + \lambda \mathcal{F}(u,v), \\ \frac{\partial v(x,t)}{\partial t} &= D \Delta^\alpha v(x,t) + \lambda \mathcal{G}(u,v), \end{aligned} \right\} \tag{2.7}$$

where $0 < \alpha \leq 2$ is termed the fractional power or mostly regarded as the anomalous diffusion exponent of the species' $u(x,t), v(x,t)$ concentrations. The parameter λ and functions \mathcal{F} and \mathcal{G} remain as earlier defined, and as illustrated in [17–19], we have

$$\Delta^\alpha u(x,t) = \frac{\partial^\alpha}{\partial t^\alpha} \nabla^2 u(x,t) = \mathcal{L}^{-1} \left\{ \frac{\partial^{\alpha-1}}{\partial t^{\alpha-1}} \nabla^2 u(x,t) \Big|_{t=0} \right\}$$

with a similar expression for v , is the generalization of the diffusion operator from standard to fractional. When solving the system with the Laplace transform, the term $\mathcal{L}^{-1} \{ \frac{\partial^{\alpha-1}}{\partial t^{\alpha-1}} \nabla^2 u(x,t) |_{t=0} \}$ actually precludes the introduction of nonphysical terms. Proceeding as earlier mentioned, a perturbation about point (u^*, v^*) results in the linearized equations

$$\left. \begin{aligned} \frac{\partial \Delta u(x,t)}{\partial t} &= \Delta^\alpha u(x,t) + \lambda(a_{11} \Delta u + a_{12} \Delta v), \\ \frac{\partial \Delta v(x,t)}{\partial t} &= D \Delta^\alpha v(x,t) + \lambda(a_{21} \Delta v + a_{22} \Delta u). \end{aligned} \right\} \tag{2.8}$$

By adopting the techniques of spatial Fourier and temporal Laplace transforms, we get

$$\begin{aligned} r \widehat{\Delta u}(k,r) - \Delta \tilde{u}(k,t=0) &= \lambda [a_{11} \widehat{\Delta u}(k,r) + a_{12} \widehat{\Delta v}(k,r)] - r^\alpha k^2 \widehat{\Delta u}(k,r), \\ r \widehat{\Delta v}(k,r) - \Delta \tilde{v}(k,t=0) &= \lambda [a_{21} \widehat{\Delta u}(k,r) + a_{22} \widehat{\Delta v}(k,r)] - r^\alpha k^2 \widehat{\Delta v}(k,r), \end{aligned}$$

which we decouple as

$$\begin{aligned} \widehat{\Delta u}(k,r) &= \frac{(r + r^\alpha D k^2 - \lambda a_{22}) \Delta \tilde{u}(k,t=0) + \lambda a_{12} \Delta \tilde{v}(k,t=0)}{(r + r^\alpha k^2 - \lambda a_{11})(r + r^\alpha D k^2 - \lambda a_{22}) - \lambda^2 a_{12} a_{21}}, \\ \widehat{\Delta v}(k,r) &= \frac{(r + r^\alpha k^2 - \lambda a_{11}) \Delta \tilde{v}(k,t=0) + \lambda a_{21} \Delta \tilde{u}(k,t=0)}{(r + r^\alpha k^2 - \lambda a_{11})(r + r^\alpha D k^2 - \lambda a_{22}) - \lambda^2 a_{12} a_{21}}. \end{aligned}$$

Thus, we obtain the conditions for the diffusion-driven case in the fractional reaction-diffusion system by finding the inverse of the Laplace transforms. So in this work, we classified the scaling of the fractional power α into subdiffusion when $0 < \alpha < 1$ [20, 21], advection flow equation when $\alpha = 1$ [19, 22], and superdiffusion when $1 < \alpha < 2$ [10, 19]. In numerical experiments, our results will be based on these classifications.

3 Fractional derivatives and adaptive numerical approaches

By replacing Fick's law for the flux U (which governs the rate at which mass is transported through an unit area against the concentration gradient) by its fractional derivative, a space-fractional diffusion equation can be derived in the form [23]

$$U = -D \Delta^\alpha u, \quad 0 < \alpha < 2, \tag{3.1}$$

with the initial function

$$u_i(x, 0) = u_{i0}(x), \quad i = 1, 2, \dots, n, \tag{3.2}$$

subject to any of the boundary conditions:

- In the case of an infinite system, $x \in (-\infty, \infty)$, here \mathbf{R} is a subset of $(-\infty, \infty)$.
- $x \in [0, L]$, $\frac{\partial u_i}{\partial x}(0, t) = \frac{\partial u_i}{\partial x}(L, t) = 0, i = 1, 2, \dots, n$, no-flux or Neumann boundary condition for a finite system.
- $x \in [0, L]$, $\mathbf{u}(0, t) = \mathbf{u}(L, t) = \mathbf{u}_a, i = 1, 2, \dots, n$, called the Dirichlet or fixed concentration boundary condition, also for a fixed system.

Here $u_i(t, \mathbf{x}) \in \mathbf{R}^n, \mathcal{F}_i : \mathbf{R}^n \rightarrow \mathbf{R}$ and D is the diffusion tensor, and $\Delta^\alpha = (\frac{\partial^\alpha}{\partial x^\alpha}, \frac{\partial^\alpha}{\partial y^\alpha}, \frac{\partial^\alpha}{\partial z^\alpha})^T$ is the Riemann-Liouville fractional gradient, for

$$\frac{\partial^\alpha}{\partial x^\alpha} u(x, y, z) = \frac{1}{\Gamma(1-\alpha)} \frac{\partial}{\partial x} \int_0^x \frac{u(s, y, z)}{(x-s)^\alpha} ds,$$

with $\frac{\partial^\alpha}{\partial y^\alpha}$ and $\frac{\partial^\alpha}{\partial z^\alpha}$ having similar expressions.

3.1 Integral representation of fractional derivative

In what follows, we shall describe the most two popular integral representation of fractional derivative via the Caputo and Riesz integral representations of the diffusion equation.

3.1.1 Caputo space-fractional derivative

A space-fractional diffusion equation takes the form

$$\frac{\partial u}{\partial t} = k_a^c D_x^\alpha u, \quad a < x < b, \tag{3.3}$$

where ${}^c D_x^\alpha$ defines the fractional derivative in the Caputo sense [10, 11]

$${}^c D_x^\alpha u(x) = \frac{1}{\Gamma(n-\alpha)} \int_a^x \left(\frac{\partial^n u(s)}{\partial s^n} \right) \frac{ds}{(x-s)^{\alpha-n+1}} \quad (n-1 < \alpha < n).$$

If we set $h = (b-a)/N, x = x_l = a + lh, u_0 = u(x-lh) = u(a), u_1 = u(x-(l-1)h) = u(a+h), \dots, u_l = u(x) = u(a+lh)$. Then we can approximate the fractional derivative term with $n = 2$ with

$$\begin{aligned} {}^c D_x^\alpha u(x) &= \frac{1}{\Gamma(2-\alpha)} \int_a^x \frac{u^{(2)}(s) ds}{(x-s)^{\alpha-1}} = \frac{1}{\Gamma(2-\alpha)} \int_0^{x-a} \frac{u^{(2)}(x-s) ds}{s^\alpha} \\ &= \frac{1}{\Gamma(2-\alpha)} \sum_{j=0}^{l-1} \int_{jh}^{(j+1)h} \frac{u^{(2)}(x-s) ds}{s^{\alpha-1}} \\ &= \frac{1}{\Gamma(2-\alpha)} \sum_{j=0}^{l-1} \frac{u(x-(j-1)h) - 2u(x-jh) + u(x-(j+1)h)}{h^2} \times \int_{jh}^{(j+1)h} \frac{ds}{s^{\alpha-1}} \\ &= \frac{h^{-\alpha}}{\Gamma(3-\alpha)} \sum_{j=0}^{l-1} (u_{l-j+1} - 2u_{l-j} + u_{l-j-1}) [(j+1)^{2-\alpha} - j^{1-\alpha}]. \end{aligned}$$

By mimicking the approach suggested in [24, 25], we can recast the fractional-in-space diffusion equation (3.3) to become an ODE,

$$\frac{du_l}{dt} = \frac{k}{h^\alpha \Gamma(3-\alpha)} \sum_{j=0}^{l-1} (u_{l-j+1} - 2u_{l-j} + u_{l-j-1}) [(j+1)^{2-\alpha} - j^{2-\alpha}],$$

for $l = 1, 2, \dots, N$, and $u_l = u(x, t)$.

3.1.2 Riesz space-fractional derivative

In a similar fashion, a space-fractional diffusion equation can be taken as

$$\frac{\partial u}{\partial t} = {}^R D_x^\alpha u, \quad a < x < b, \tag{3.4}$$

where ${}^R D_x^\alpha$ is the Riesz fractional derivative, with expression

$${}^R D_x^\alpha = -(-\Delta)^{\alpha/2} = \frac{d^\alpha}{d|x|^\alpha} = -{}_x I_0^{-\alpha}$$

and

$${}_x I_0^{-\alpha} u(x) = C_-(\alpha) {}_x I_+^\alpha u(x) + C_+(\alpha) {}_x I_-^\alpha u(x).$$

In this sense, ${}_x I_\pm^{-\alpha}$ is used to represent the Riemann-Liouville (or Weyl) fractional integrals, defined as

$$\begin{aligned} {}_x I_+^{-\alpha} u(x) &= \frac{1}{\Gamma(\alpha)} \int_a^x \frac{u(s) ds}{(x-s)^{1-\alpha}}, \\ {}_x I_-^{-\alpha} u(x) &= \frac{1}{\Gamma(\alpha)} \int_x^b \frac{u(s) ds}{(s-x)^{1-\alpha}}, \\ C_-(\alpha) &= C_+(\alpha) = \frac{1}{2 \cos(\frac{\pi\alpha}{2})}, \end{aligned}$$

and, recovering the Riesz potential, we have

$${}_x I_0^{-\alpha} u(x) = \frac{1}{2\Gamma(\alpha) \cos(\frac{\pi\alpha}{2})} \int_a^b \frac{u(s) ds}{|x-s|^{1-\alpha}}.$$

In the interval $1 < \alpha < 2$, which corresponds to the superdiffusive scenario, we define the pseudo-differential operator as

$${}_x D_0^\alpha = -(C_+(\alpha) {}_x D_+^\alpha + C_-(\alpha) {}_x D_-^\alpha).$$

The integral operator ${}_x I_\pm^\alpha$ is represented by ${}_x I_\pm^\alpha = \frac{d^2}{dx^2} ({}_x I_\pm^{2-\alpha})$, so that

$$\begin{aligned} {}_x D_+^\alpha u &= \frac{d^2}{dx^2} ({}_x I_+^{2-\alpha}) u = \frac{u(a)(x-a)^{-\alpha}}{\Gamma(1-\alpha)} + \frac{u'(a)(x-a)^{1-\alpha}}{\Gamma(2-\alpha)} + \frac{1}{\Gamma(2-\alpha)} \int_a^x \frac{u^{(2)}(s) ds}{(x-s)^{\alpha-1}}, \\ {}_x D_-^\alpha u &= \frac{d^2}{dx^2} ({}_x I_-^{2-\alpha}) u = \frac{u(b)(b-x)^{-\alpha}}{\Gamma(1-\alpha)} - \frac{u'(b)(b-x)^{1-\alpha}}{\Gamma(2-\alpha)} + \frac{1}{\Gamma(2-\alpha)} \int_x^b \frac{u^{(2)}(s) ds}{(s-x)^{\alpha-1}}. \end{aligned}$$

In the spirit of Liu *et al.* [24, 25], we have the following equivalent ODE for (3.4):

$$\begin{aligned} \frac{du_l}{dt} = & -\frac{1}{2\Gamma(\alpha)\cos(\frac{\pi\alpha}{2})}\frac{kh^{-\alpha}}{\Gamma(3-\alpha)}\left\{\frac{(1-\alpha)(2-\alpha)u_0}{l^\alpha} + \frac{(2-\alpha)}{l^{\alpha-1}}(u_1-u_0)\right. \\ & + \sum_{j=0}^{l-1}(u_{l-j+1}-2u_{l-j}+u_{l-j-1})[(j+1)^{2-\alpha}-j^{2-\alpha}] + \frac{(1-\alpha)(2-\alpha)u_N}{(N-l)^\alpha} \\ & \left. - \frac{(2-\alpha)}{(N-l)^{(\alpha-1)}}(u_N-u_{N-1}) + \sum_{j=0}^{N-l-1}(u_{l+j-1}-2u_{l+j}+u_{l+j+1})[(j+1)^{2-\alpha}-j^{2-\alpha}]\right\}. \end{aligned}$$

Many others integral representations of the fractional derivatives are well classified in [1, 2, 4, 9–11, 21, 26].

3.2 Numerical techniques for fractional diffusion equation

In this section, we do not intend to go into details, but we report a brief survey of some of the numerical approaches that have been used. Several numerical techniques have been used in the literature to circumvent the non-local restrictions associated with the space-fractional operators. Some of these methods include finite element, finite difference and spectral methods, to mention a few.

3.2.1 Finite difference method

Over the years, many time dependent partial differential equations have combined low-order nonlinear with higher-order linear terms. Until now, numerical simulation of most physical models still relied on a low-order finite difference scheme to discretize both the space- and time-fractional-order derivatives, which are largely encountered in the fields of computational physics and mathematics. While the finite difference scheme remains simple, straightforward and easy-to-code for the integration of integer-order (classical) differential equations, its applicability is reduced for fractional-order differential equations as it results to systems of linear equation defined by dense or large full matrices.

A finite difference (FD) discretization of the fractional-order differential equation can be obtained by using the well-known shifted Grünwald-Letnikov approximation of the Riemann-Liouville derivatives [1, 27, 28]. Here, we provide a further approximation by applying the FD method to solving the space-fractional diffusion equation

$$\frac{\partial u}{\partial t} = D(\Delta)^\alpha u, \quad 1 < \alpha < 2, \tag{3.5}$$

subject to the boundary conditions $u(0, t) = u(1, t) = 0$ and the initial function $u(x, 0) = f(x)$ in one-dimension. We consider the cases $0 < \alpha < 1$ and $1 < \alpha < 2$ useful for many applications. The scenario of non-integer $1 < \alpha < 2$ is used to model the superdiffusive case in which a cloud of particles spreads at a faster rate than in the classical diffusion model. It should be noted that we have the classical advective flow equation when $\alpha = 1$ and standard diffusion equation whenever $\alpha = 2$.

By using the FD method to approximate space derivatives first in the classical medium $\alpha = 2$, equation (3.5) can be written in the matrix form

$$\frac{d\mathbf{u}}{dt} = \delta\mathbf{A}\mathbf{u}, \tag{3.6}$$

where $\delta = D/h^2$ and

$$\mathbf{A} = \begin{pmatrix} 2 & -1 & & & \\ -1 & 2 & -1 & & \\ & -1 & 2 & -1 & \\ & & \ddots & \ddots & -1 \\ & & & -1 & 2 \end{pmatrix}, \quad \mathbf{u} = \begin{pmatrix} u_1 \\ u_2 \\ \vdots \\ u_{N-2} \\ u_{N-1} \end{pmatrix}. \tag{3.7}$$

We take \mathbf{A}/h^2 to be approximation of differential operator $T = \partial^2/\partial x^2$, then we set $m(T^{\alpha/2}) \approx 1/h^\alpha \mathbf{A}^\alpha$ (an approximate matrix representation of T) and we approximate (3.5) by the equation

$$\frac{d\mathbf{u}}{dt} = \bar{\delta} \mathbf{A}^\alpha \mathbf{u}, \tag{3.8}$$

with $\bar{\delta} = D/h^\alpha$. The solution of fractional-in-space diffusion (3.8) is given by $\mathbf{u}(t) = \exp(\bar{\delta} \mathbf{A}^\alpha t) \mathbf{u}(0)$. But if \mathbf{A} is a symmetric positive definite matrix, the solution of (3.8) takes the form

$$\mathbf{u}(t) = \mathbf{B} \exp(\bar{\delta} \Lambda^\alpha t) \mathbf{B}^T \mathbf{u}(0),$$

where

$$\exp(\bar{\delta} \Lambda^\alpha t) = \text{diag}(\exp(\bar{\delta} \lambda_1^\alpha t), \exp(\bar{\delta} \lambda_2^\alpha t), \dots, \exp(\bar{\delta} \lambda_{N-1}^\alpha t)) \quad \text{and}$$

$$\Lambda = \text{diag}(\lambda_1, \lambda_2, \dots, \lambda_{N-1})$$

are the eigenvalues of \mathbf{A} , $\mathbf{B} \in \mathbb{R}^{(N-1) \times (N-1)}$.

3.2.2 Finite element method

With the finite element method, the exact solution is usually approximated with expansion in terms of piecewise polynomials $\phi_j(x)$:

$$u(x, t) \approx \sum_{j=1}^N u_j(t) \phi_j(x).$$

The basis function $\phi_j(x)$ has a compact support which corresponds to the node j of a mesh (or grid) that divides the computational domain in $N - 1$ segments with step-length $h = L/(N - 1)$. The position of node j is denoted x_j , and computing the fractional derivative of the solution then amounts to computing the fractional derivative of all basis functions $\phi_j(x)$; see Hanert [29, 30] for details.

The major advantage of adopting a finite element technique is due to the flexibility it offers. For instance, the ability to model complex geometries, and to use local refinement to improve approximations. The main obstacle to circumvent is the non-local nature of the fractional operator, and direct application of finite element would result in a large and dense matrix [31]. The construction of such a matrix often results in serious difficulties, particularly in efficiency. When using a finite element technique to approximate a fractional Laplacian operator, it is not a trivial exercise to obtain reliable results, because of

the dense matrix structure; to get optimal convergence would tremendously amount to an increase in the radius of truncation [27, 32].

3.2.3 Fourier spectral method

A little attention has been given to spectral method despite its desired ability to achieve higher-order convergence (accuracy and efficiency) over the existing low-order schemes such as finite difference and finite element schemes when applied to solve fractional-in-space reaction-diffusion equations. Application of spectral methods for the solution of classical reaction-diffusion problems is considered to be relatively simple and, being a subject of mathematical and theoretical studies for some years, has been by now examined almost completely. However, the case of fractional-order reaction-diffusion is still poorly understood with just a handful of papers addressing the problems with spectral methods. Some of the little work done on spectral methods is [19, 32–34].

For spectral representation, we let H be the real Hilbert space in $\mathcal{L}_2(0, L)$, and consider the operator $T : \mathcal{H} \rightarrow H$ defined by $T\varphi = \Delta\varphi = \frac{d^2\varphi}{dx^2}$ on $\mathcal{H} = \{\varphi \in H; \varphi', \varphi'' \in \mathcal{L}_2(0, L) \text{ are continuous with boundary condition } \mathcal{B}(\varphi) = 0\}$. Then $T\varphi_n = \lambda_n\varphi_n, n = 1, 2, \dots$. For any $\varphi \in H$,

$$\varphi = \sum_{n=1}^{\infty} c_n\varphi_n, \quad c_n = \langle \varphi, \varphi_n \rangle \quad \text{and} \quad T\varphi = \sum_{n=1}^{\infty} \lambda_n c_n \varphi_n.$$

So, if ϖ is a continuous function on \mathbb{R} , then

$$\varpi(T)\varphi = \sum_{n=1}^{\infty} \varpi(\lambda_n) c_n \varphi_n, \tag{3.9}$$

provided $\sum_{n=1}^{\infty} |\varpi(\lambda_n) c_n|^2 < \infty$.

For the space discretization, we consider the one-dimensional fractional-in-space diffusion equation (3.5) above, subject to initial condition $u(x, 0) = u_0(x)$ and homogeneous boundary conditions clamped at the extreme ends of spatial domain $x \in [a, b]$. By relating (3.9) with the technique in [35], the fractional Laplacian $(\Delta)^\alpha$ can be defined in the space of functions

$$H_0^\alpha(\Omega) = \left\{ u = \sum_{j=0}^{\infty} a_j \lambda_j^\alpha \in L^2(\Omega) : \|u\|_{H_0^\alpha(\Omega)} = \left(\sum_{j=0}^{\infty} a_j^2 \lambda_j^\alpha \right)^{1/2} < \infty \right\}, \tag{3.10}$$

where

$$\|u\|_{H_0^\alpha(\Omega)} = \|(\Delta)^\alpha u\|_{L^2(\Omega)}. \tag{3.11}$$

Therefore for any $u \in H_0^\alpha$, the Laplacian $(\Delta)^\alpha$ is defined by

$$\Delta^\alpha u = \sum_{i=0}^{\infty} a_i \lambda_i^\alpha \varphi_i, \tag{3.12}$$

where φ_j and λ_j will depend on the specified boundary conditions.

For homogeneous Dirichlet boundary condition we obtain

$$(\varphi_j, \lambda_j) = \left(\left[\frac{(j+1)\pi}{b-a} \right]^2, \sqrt{\frac{2}{b-a}} \sin \left[\frac{(x-a)\pi(j+1)}{b-a} \right] \right), \tag{3.13}$$

and for homogeneous Neumann boundary condition we get

$$(\varphi_j, \lambda_j) = \left(\left[\frac{\pi j}{b-a} \right]^2, \sqrt{\frac{2}{b-a}} \sin \left[\frac{(x-a)\pi j}{b-a} \right] \right). \tag{3.14}$$

Next, we want to extend this approach to higher-dimensional two-component fractional-in-space reaction-diffusion system (2.7) in the presence of reaction (source) terms; by applying the fast Fourier transform we obtain

$$\begin{aligned} U_t(\omega_x, \omega_y, t) &= \delta_1(\omega_x^\alpha + \omega_y^\alpha)U(\omega_x, \omega_y, t) + \mathcal{F}[f(u(x, y, t), v(x, y, t))], \\ V_t(\omega_x, \omega_y, t) &= \delta_2(\omega_x^\alpha + \omega_y^\alpha)V(\omega_x, \omega_y, t) + \mathcal{G}[g(u(x, y, t), v(x, y, t))], \end{aligned}$$

where U and V are the double Fourier transforms for species $u(x, y, t)$ and $v(x, y, t)$. In other words,

$$\begin{aligned} \mathcal{F}[u(x, y, t)] &= U(\omega_x, \omega_y, t) = \int_0^\infty \int_0^\infty u(x, y, t) e^{-i(\omega_x x + \omega_y y)} dx dy, \\ \mathcal{G}[v(x, y, t)] &= V(\omega_x, \omega_y, t) = \int_0^\infty \int_0^\infty v(x, y, t) e^{-i(\omega_x x + \omega_y y)} dx dy. \end{aligned}$$

With $\Omega^\alpha = \omega_x^\alpha + \omega_y^\alpha$, we explicitly remove the issue of stiffness in the linear piece using integrating factors, by setting

$$U = e^{\delta_1 \Omega^\alpha t} \bar{U}, \quad V = e^{\delta_2 \Omega^\alpha t} \bar{V},$$

such that

$$\begin{aligned} \partial_t \bar{U} &= e^{\delta_1 \Omega^\alpha t} \mathcal{F}[f(u, v)], \\ \partial_t \bar{V} &= e^{\delta_2 \Omega^\alpha t} \mathcal{G}[g(u, v)]. \end{aligned} \tag{3.15}$$

At this point, we can now discretize the square domain on equi-spaced number of points N_x and N_y in the spatial directions x and y . We adapt the discrete fast Fourier transform (DFFT) [35] to transform (3.15) to a system of ODEs

$$\begin{aligned} \partial_t \bar{U}_{i,j} &= e^{K_u \Omega_{i,j}^\alpha t} \mathcal{F}[f(u_{i,j}, v_{i,j}, w_{i,j})], \\ \partial_t \bar{V}_{i,j} &= e^{K_v \Omega_{i,j}^\alpha t} \mathcal{G}[g(u_{i,j}, v_{i,j}, w_{i,j})], \end{aligned} \tag{3.16}$$

where $u_{i,j} = u(x_i, y_j)$, $v_{i,j} = v(x_i, y_j)$ and $\Omega_{i,j}^\alpha = \chi_x^\alpha(i) + \chi_y^\alpha(j)$. Boundary conditions are now clamped at the ends of the domain. At this junction, the whole system has been converted to ODEs, the stiffness property associated with the spatial derivatives is gone. It should be noted that any explicit higher-order scheme can be employed to advance in time. High

order time integration methods can be naturally used in conjunction with high resolution spectral methods to obtain efficient and accurate approximations of the phase field models.

3.2.4 Time stepping method

For the temporal discretization, we employ the modified Krogstad [36, 37] version of the exponential time differencing Runge-Kutta method that was earlier proposed by Cox and Matthews [38]. It reads

$$\begin{aligned}
 W_{n+1} = e^{L dt} W_n + \gamma_1 \mathbf{N}(W_n, t_n) + \gamma_2 \left[\mathbf{N}\left(a_n, t_n + \frac{dt}{2}\right) + \mathbf{N}\left(b_n, t_n + \frac{dt}{2}\right) \right] \\
 + \gamma_3 \mathbf{N}\left(c_n, t_n + \frac{dt}{2}\right), \tag{3.17}
 \end{aligned}$$

where $W = W(u, v)$, \mathbf{L} , \mathbf{N} defined as linear and nonlinear operators with variable coefficients

$$\begin{aligned}
 a_n &= e^{L \frac{dt}{2}} W_n + \mathbf{L}^{-1} (e^{L \frac{dt}{2}} - \mathbf{I}) \mathbf{N}(W_n, t_n), \\
 b_n &= e^{L \frac{dt}{2}} W_n + \mathbf{L}^{-1} (e^{L \frac{dt}{2}} - \mathbf{I}) \mathbf{N}\left(a_n, t_n + \frac{dt}{2}\right), \\
 c_n &= e^{L \frac{dt}{2}} a_n + \mathbf{L}^{-1} (e^{L \frac{dt}{2}} - \mathbf{I}) \left[2\mathbf{N}\left(b_n, t_n + \frac{dt}{2}\right) - \mathbf{N}(W_n, t_n) \right], \tag{3.18}
 \end{aligned}$$

and the constants

$$\begin{aligned}
 \gamma_1 &= dt^{-2} \mathbf{L}^{-3} [-4 - \mathbf{L} dt + e^{L dt} (4 - 3\mathbf{L} dt + (\mathbf{L} dt)^2)], \\
 \gamma_2 &= 2 dt^{-2} \mathbf{L}^{-3} [2 + \mathbf{L} dt + e^{L dt} (-2 + \mathbf{L} dt)], \\
 \gamma_3 &= dt^{-2} \mathbf{L}^{-3} [-4 - 3\mathbf{L} dt - (\mathbf{L} dt)^2 + e^{L dt} (4 - \mathbf{L} dt)]. \tag{3.19}
 \end{aligned}$$

To overcome the pronounced cancelation errors associated with the higher-order exponential time differencing Runge-Kutta method, the three coefficients in (3.19) suffer serious cancelation errors when the eigenvalues of \mathbf{L} are close to zero. The vulnerability cancelation errors in the higher-order variants can render the whole schemes useless. As a result, modified exponential time differencing (ETD) schemes are proposed by using the complex contour integrals

$$f(\mathbf{L}) = \frac{1}{2\pi i} \int_{\Gamma} f(t)(t\mathbf{I} - \mathbf{L})^{-1} dt$$

here Γ is the contour that encloses the eigenvalues of l [39]. Details of derivation and stability analysis of scheme (3.17), which we denote for brevity in this paper ETD4RK, can be found in [13, 19, 37–43]. In the past, ETD schemes have also been used by some authors under different names [44–46].

3.2.5 Convergence analysis

Here, by convergence analysis we examined the trade-off between the finite difference and Fourier spatial discretizations in terms of accuracy and efficiency. We test the performance

of the schemes by reporting the error norm ℓ_∞ in the numerical experiment at $t = 2$ as

$$\ell_\infty(N) = \max_{1 \leq j \leq N} \frac{|u_j - \tilde{u}_j|}{|u_j|}, \tag{3.20}$$

where \tilde{u} and u are the respective approximate and exact solutions, and N is the number of computational grids.

By using (3.10 and (3.12), a straightforward analytical solution of (3.5) can be presented as

$$u(x, t) = \sum_{j=0}^{\infty} \tilde{u}_j(t) \varphi_j(x) = \sum_{j=0}^{\infty} \tilde{u}_j(0) \exp(-D\lambda_j^\alpha t) \varphi_j(x), \tag{3.21}$$

with $\tilde{u}_j(0) = \langle u_0(x), \varphi_j(x) \rangle$. Eigenvalues and eigenfunctions will depend on any of the given boundary conditions (3.13) and (3.14). Fourier spectral methods denote the truncated series expansion of (3.21) when a finite number of orthonormal trigonometric eigenfunctions $\{\varphi_j\}$ are considered, that is,

$$u(x, t) \approx \sum_{j=0}^{N-1} \tilde{u}_j(t) \varphi_j(x) = \sum_{j=0}^{N-1} \tilde{u}_j(0) \exp(-D\lambda_j^\alpha t) \varphi_j(x). \tag{3.22}$$

For the space convergence, the solution of diffusion equation (3.5) using a finite difference or finite element matrix-based technique can be approximated by

$$\mathbf{u}(t) \approx \mathbf{L} \text{diag} \{ \exp(-D\lambda_0^\alpha t), \exp(-D\lambda_1^\alpha t), \dots, \exp(-D\lambda_{N-1}^\alpha t) \} \mathbf{L}^{-1} \mathbf{u}_0, \tag{3.23}$$

where \mathbf{L} denotes the corresponding eigenvectors matrix, and \mathbf{u} represents the vector node of u [32, 47]. Obviously, both (3.22) and (3.23) are exact in time, to study the convergence of the two schemes used for numerical approximation of (3.5) we proceed by using a simple example. Hence, we consider for simplicity a one-dimensional fractional-in-space diffusion benchmark problem with simple source term [10, 14, 32], which consists of finding $u(x, t)$ such that

$$\frac{\partial u(x, t)}{\partial t} = D\Delta^\alpha + f(x, t), \quad x \in [0, 1], t > 0, \tag{3.24}$$

where

$$f(x, t) = \frac{D}{4} t^\alpha \{ 3[1 + (2\pi)^\alpha] \sin(2\pi x) - [1 + (6\pi)^\alpha] \sin(6\pi x) \} + \alpha t^{\alpha-1} \sin^3(2\pi x) - Du,$$

with initial condition computed as $u(x, 0) = \text{zeros}(N, 1)$, $u(0, t) = 0$, $u(1, t) = 0$ and the diffusion constant $D > 0$. The exact solution is given by $u(x, t) = t^\alpha \sin^3(2\pi x)$.

Convergence results for finite differences and Fourier spectral methods are at varying α are displayed in Figure 1 (a – b), respectively. Also in Figure 1, we present the numerical results justifying the performance of both finite difference and Fourier spectral methods at some instances of α . Panel (c) shows the comparison between the exact (solid-lines) and numerical (superimposed stars, circle and crosses) solutions for $\alpha = (0.5, 1.1, 1.5)$. Plot (d)

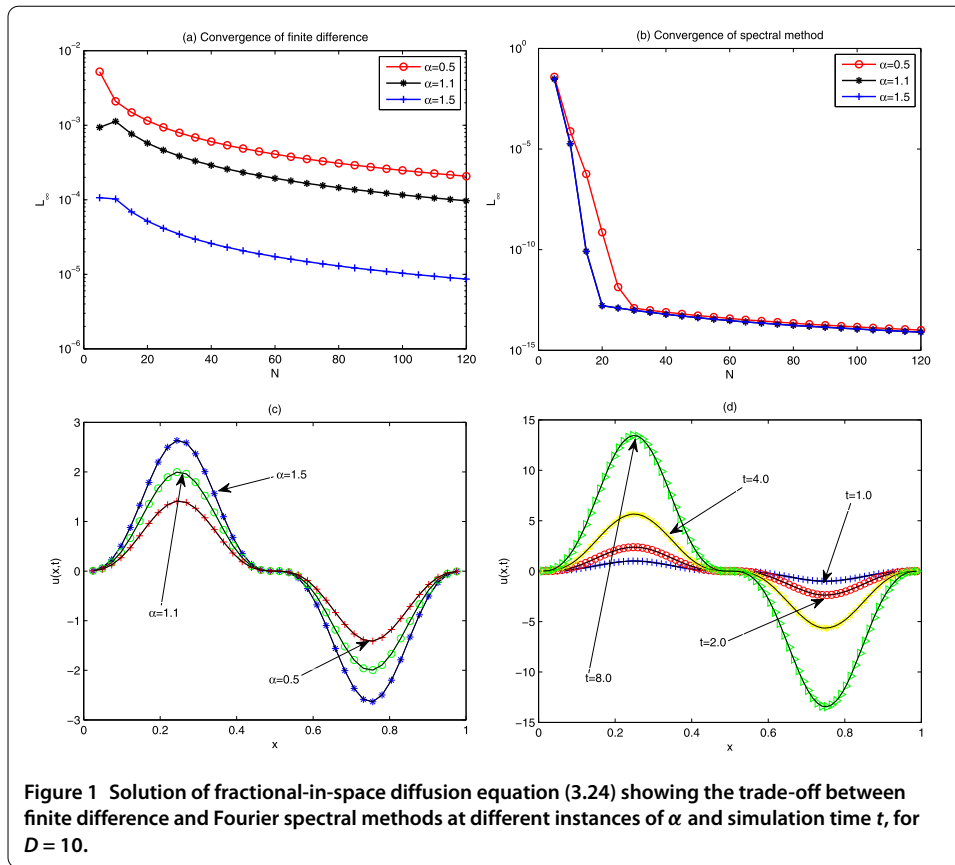


Figure 1 Solution of fractional-in-space diffusion equation (3.24) showing the trade-off between finite difference and Fourier spectral methods at different instances of α and simulation time t , for $D = 10$.

Table 1 The relative error for fractional diffusion equation for various values of discretization, at $D = 0.25$ and $t = 5$

N	40	50	60	70	80
Fourier spectral	1.2894e-08	1.5238e-08	2.2660e-08	3.1952e-08	4.1239e-08
Finite difference	1.0017e-04	3.9125e-04	2.6447e-03	2.9589e-03	1.4286e-02
Ratio	7.7687e+03	2.5676e+04	1.1671e+05	9.2605e+04	3.4642e+05

is obtained at different instances of time $t = (1, 2, 4, 8)$ at fractional value $\alpha = 1.25$. Comparison in panels (a) and (b) for $t = 1$ and the relative error results in Table 1 justify well enough abandoning the finite difference method in the remaining part of this work.

4 Numerical experiments

In this section, we illustrate the mathematical techniques presented in the previous sections with some numerical examples in one, two, and probably three dimensions. We first consider the fractional-in-space reaction-diffusion system (2.7) and focus on the re-scaled Beddington-DeAngelis functional response with logistic growth term [48–51],

$$\mathcal{F}(u, v) = \sigma u(1 - u)(\beta + u + v) - uv, \quad \mathcal{G}(u, v) = \gamma uv - \delta v(\beta + u + v). \quad (4.1)$$

In order to give a good working guideline on the appropriate choice of parameters when numerically simulating the full fractional reaction-diffusion system, it is necessary to consider the local dynamics of the system [52]. By considering the nullclines $\mathcal{F}(u, v) = 0$ and

$\mathcal{G}(u, v) = 0$, it is not difficult to see that model (2.7) with kinetics (4.1) possesses three equilibrium points in the absence of diffusion. The first point when $(u^*, v^*) = (0, 0)$ corresponds to total washout of both populations, while $(u^*, v^*) = (1, 0)$ or vice versa corresponds to existence of one population. The third equilibrium point

$$(u^*, v^*) = \left(\frac{\sigma\gamma - \gamma + \delta + \sqrt{(\sigma\gamma - \gamma + \delta)^2 + 4\sigma\gamma\delta\beta}}{2\sigma\gamma}, \left(\frac{\gamma}{\delta} - 1 \right) u^* - \beta \right)$$

is a trivial state which corresponds to the coexistence of both prey and predator. It is the dynamics in the biologically meaningful region $u \geq 0, v \geq 0$ which is of great interest.

The Jacobian or community matrix that corresponds to the interior equilibrium point (u^*, v^*) is given by

$$J = \begin{pmatrix} a_{11} & a_{12} \\ a_{21} & a_{22} \end{pmatrix} = \begin{pmatrix} \sigma\mathcal{A}\mathcal{B} - \sigma u^*\mathcal{B} + \sigma u^*\mathcal{A} - v^* & \sigma u^*\mathcal{A} - u^* \\ \gamma v^* - \delta v^* & \gamma u^* - \delta\mathcal{B} - \delta v^* \end{pmatrix} \tag{4.2}$$

where $\mathcal{A} = (1 - u^*)$ and $\mathcal{B} = (\beta + u^* + v^*)$. To ensure that the point (u^*, v^*) satisfies $|J(u^*, v^*)| > 0$, it is necessary to keep β in the interval $(0, \frac{\gamma - \delta}{\delta})$ when numerically simulating the full system.

For the second example, we shall focus on the specific type II functional response [53],

$$\mathcal{F}(u, v) = u(1 - u) - \frac{uv}{u + \sigma}, \quad \mathcal{G}(u, v) = \frac{\beta uv}{u + \sigma} - \gamma v. \tag{4.3}$$

The equilibrium point (u^*, v^*) corresponding to the existence of both species is given by

$$u^* = \frac{\sigma\gamma}{\beta - \gamma}, \quad v^* = (1 - u^*)(u^* + \sigma), \quad \beta > \gamma \text{ and } \sigma < \frac{\beta - \gamma}{\gamma}.$$

Details of the linear stability analysis of kinetics (4.3) can be found in [52, 53].

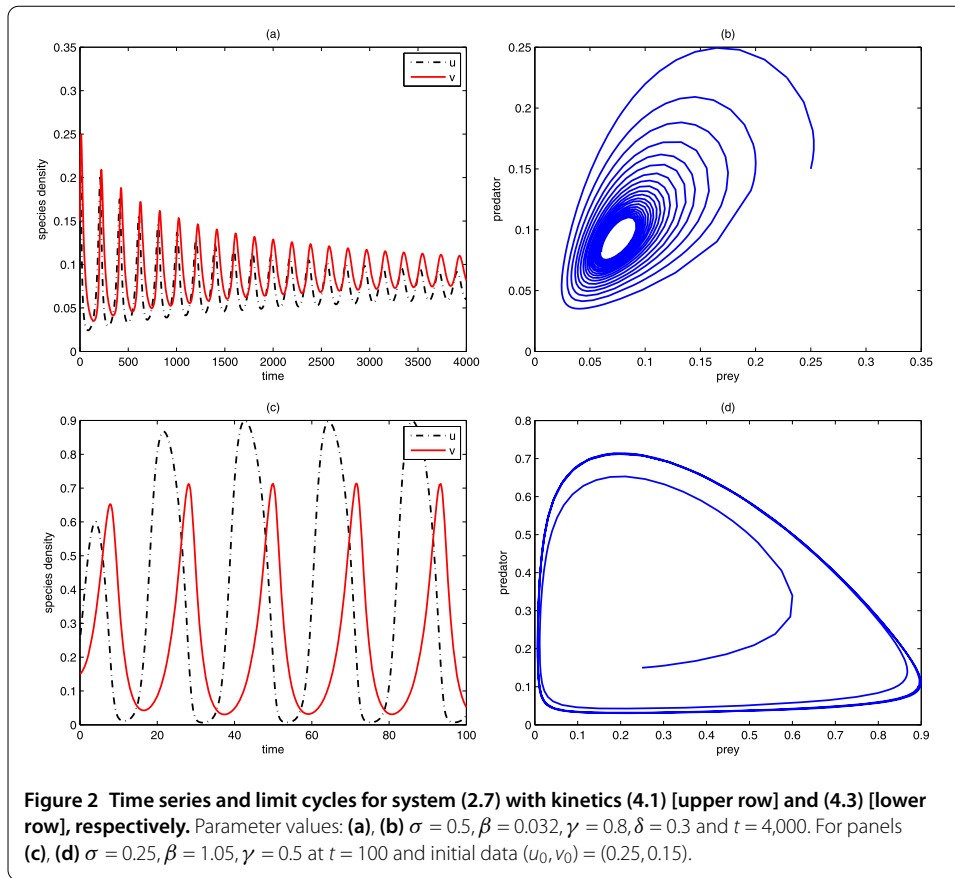
It is clear from the results obtained in Figure 2 that the two species oscillate in phase. The populations profile in (a) which correspond to the coexistence of the species are unstable with initial time but become stable as time is increasing. It is otherwise with kinetics (4.3) in plot (c), where the species are stable with initial time and become unstable with spatio-temporal oscillations at bigger time, say $t = 1,000$.

4.1 Two-dimensional results

In order to give a better illustration of the theoretical results and some biological wave phenomena of the fractional-in-space system describing spatial predator-prey interactions, we present in this subsection some numerical results in two space dimensions (2D). We let $x, y \in \mathbf{R}^2, \Delta^\alpha = (\partial^\alpha / \partial x^\alpha + \partial^\alpha / \partial y^\alpha)$ and experiment on a growing domain in the interval $[-L, L]$ subject to Neumann boundary conditions clamped at the domain extreme ends, and initial conditions specifically chosen as

$$\begin{aligned} u(x, y, 0) &= 1 - \exp(-20((x - 1/2)^2 + (y - 1/2)^2)), \\ v(x, y, 0) &= \exp(-20((x - 1/2)^2 + (y - 1/2)^2)), \end{aligned} \tag{4.4}$$

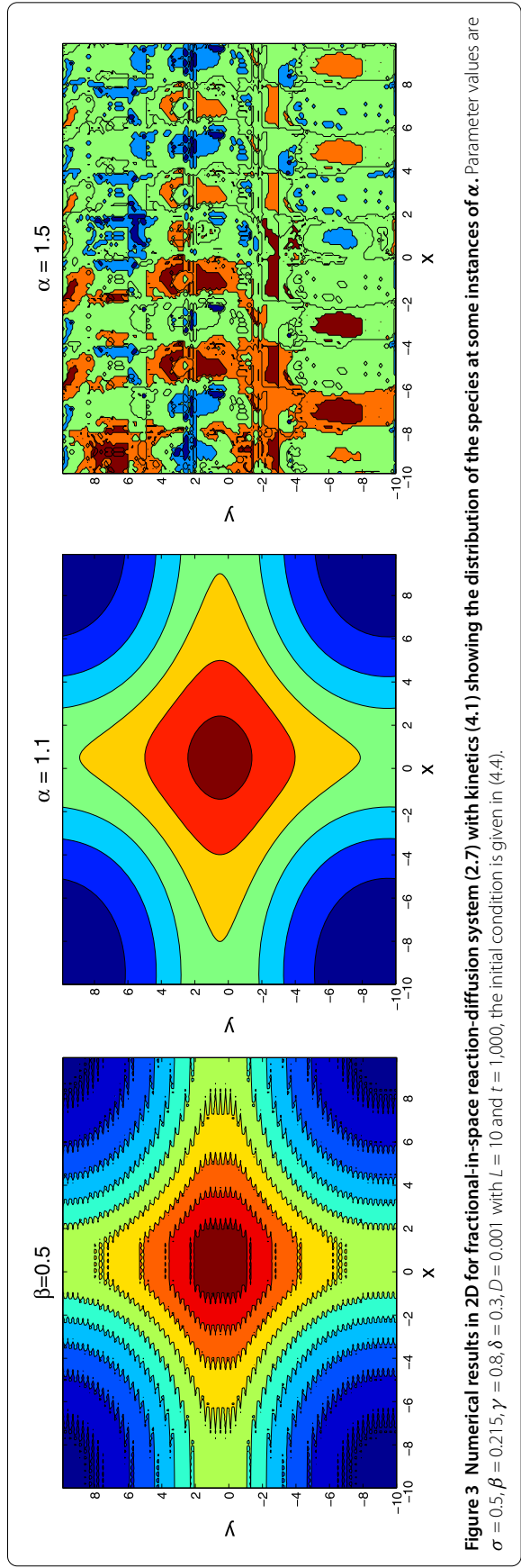
so as to induce a nontrivial spatio-temporal dynamics.



In the experiment with kinetics (4.1), it was found that the two species have similar pattern distributions. As a result, we report only that of species u as shown in Figure 3. The effects of fractional power α are shown to be more pronounced in the subdiffusive case when $\alpha = 0.5$ and superdiffusive scenario at $\alpha = 1.5$. The unsteady oscillatory patterns indicate the presence of a Turing instability. The evolution of more complex spiral patterns is shown in Figure 4 for kinetics (4.3) at different instances of fractional index α at time $t = 1,000$. The upper and lower rows represents the distribution patterns of species u and v , respectively, with varying values of α . We further report some complex spiral patterns distribution for v in Figure 5 in the fractional regime $1 < \alpha < 2$, which we classify as a superdiffusive case. It should be mentioned that other Turing patterns can be observed, depending on the choice of initial and parameter values.

4.2 Three-dimensional results

In the spirit of [54–56], we further explore some of the dynamic richness of fractional-in-space reaction-diffusion, we extend our numerical experiments to three space dimensions (3D). As usual, we let $x, y, z \in \mathbf{R}^3, \Delta^\alpha = (\partial^\alpha / \partial x^\alpha + \partial^\alpha / \partial y^\alpha + \partial^\alpha / \partial z^\alpha)$ denote the Laplacian operator with fractional order α . As discussed in Section 3, our numerical simulation results apply to general boundary conditions, but for the sake of ease of exposition we first experiment on a growing domain of size $[-L, L]$ subject to Neumann boundary conditions and also consider a solution in the domain size $[0, L]$ subject to the Dirichlet or fixed boundary



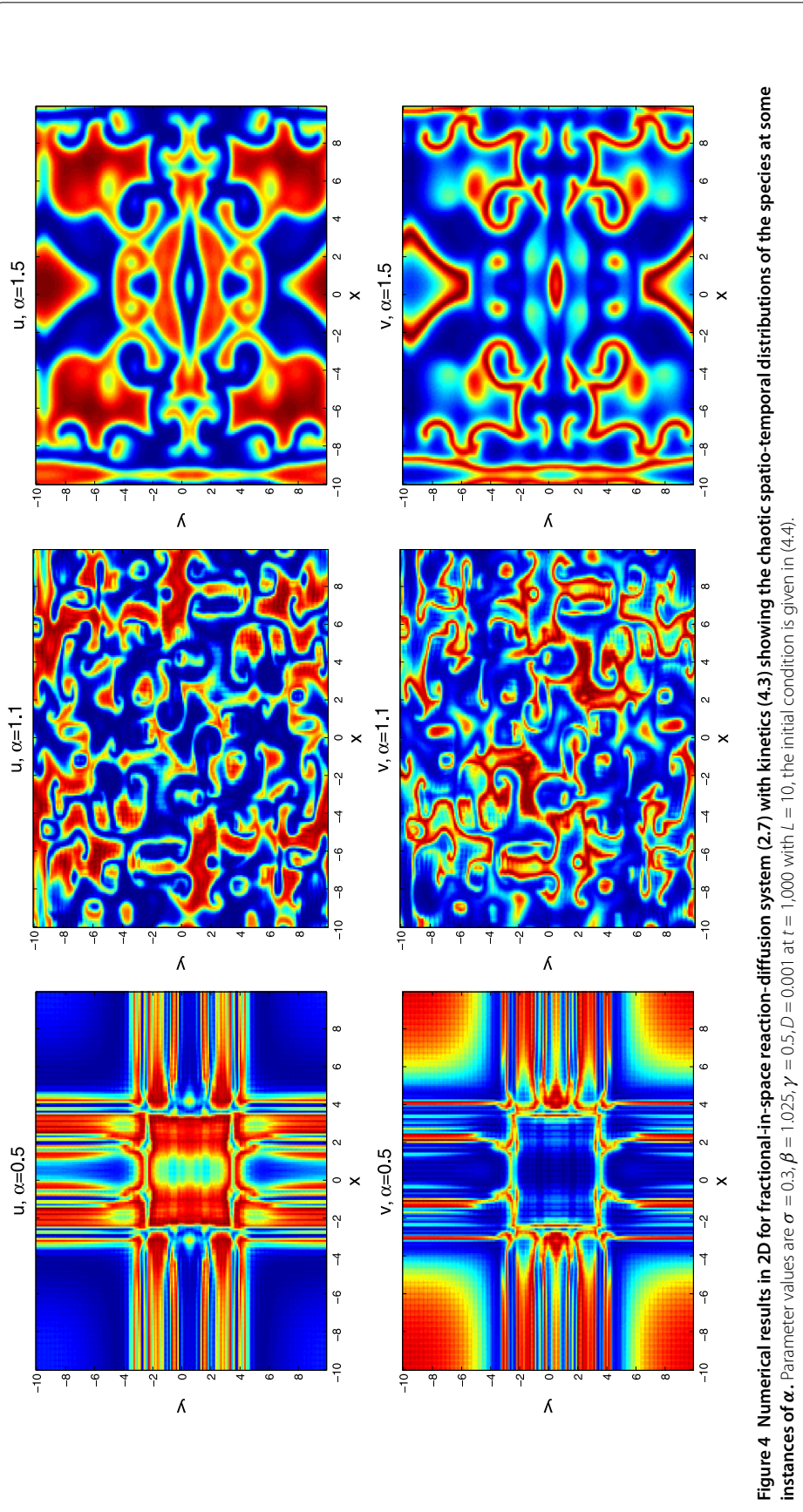
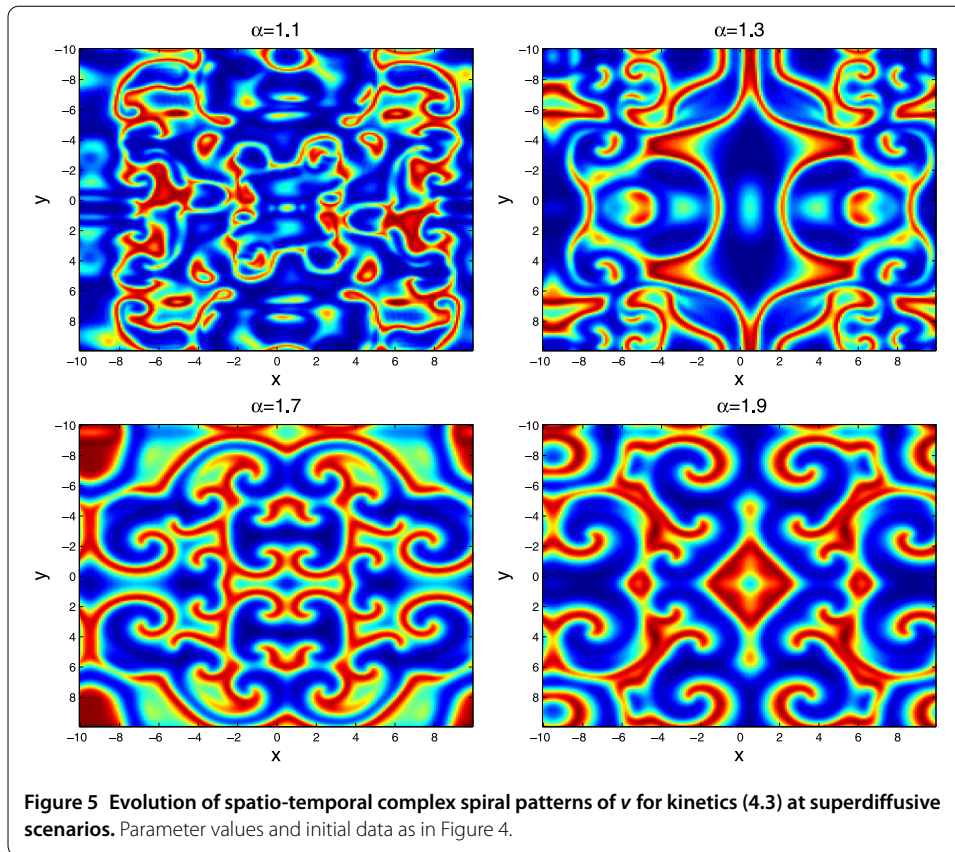


Figure 4 Numerical results in 2D for fractional in-space reaction-diffusion system (2.7) with kinetics (4.3) showing the chaotic spatio-temporal distributions of the species at some instances of α . Parameter values are $\sigma = 0.3, \beta = 1.025, \gamma = 0.5, D = 0.001$ at $t = 1,000$ with $L = 10$, the initial condition is given in (4.4).



condition. For both kinetics, we focus on the initial functions

$$\begin{aligned}
 u(x, y, z, 0) &= 1 - 0.5 \exp(-10((x - s/2)^2 + (y - s/2)^2 + (z - s/2)^2)), \\
 v(x, y, z, 0) &= 0.25 \exp(-10((x - s/2)^2 + (y - s/2)^2 + (z - s/2)^2)), \quad s = 1.
 \end{aligned}
 \tag{4.5}$$

In Figure 6, we observed different amazing patterns for the distributions of species v . We considered two important boundary conditions to explore the variability in 3D patterns for the fractional-in-space reaction-diffusion system. We should also inform the reader that other pattern scenarios are possible and subject to the choice of initial functions, boundary conditions, fractional power index value and the domain size.

Similarly in Figure 7, we experiment with system (2.7) with kinetics (4.3). It was also found that the distributions of species u and v are almost of the same type. As a result, we present the evolutions of species u in 3D with both Neumann and Dirichlet boundary conditions as shown in the upper and lower rows, respectively. Other patterns are possible depending on the choice of parameters and initial conditions.

5 Conclusion

For many years, the finite difference method has been considered as the mainstay in the numerical treatment of nonlinear partial differential equations. In this paper, we introduce the Fourier spectral method as a better alternative approach to the finite difference scheme, which is capable of removing the stiffness issues associated with the non-integer-order spatial derivative of fractional reaction-diffusion equations. For the temporal dis-

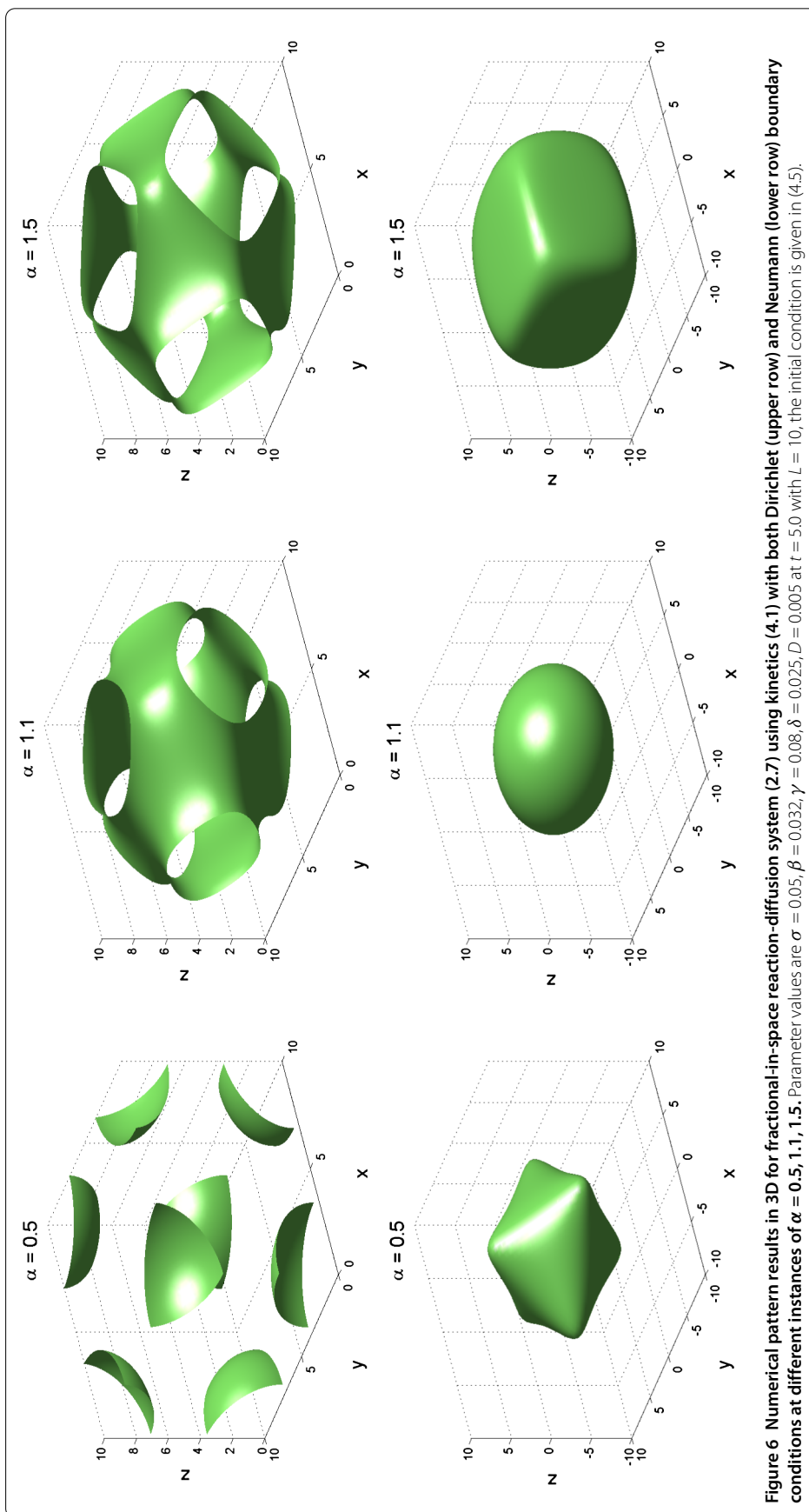


Figure 6 Numerical pattern results in 3D for fractional-in-space reaction-diffusion system (2.7) using kinetics (4.1) with both Dirichlet (upper row) and Neumann (lower row) boundary conditions at different instances of $\alpha = 0.5, 1.1, 1.5$. Parameter values are $\sigma = 0.05, \beta = 0.032, \gamma = 0.08, \delta = 0.025, D = 0.005$ at $t = 5.0$ with $L = 10$, the initial condition is given in (4.5).

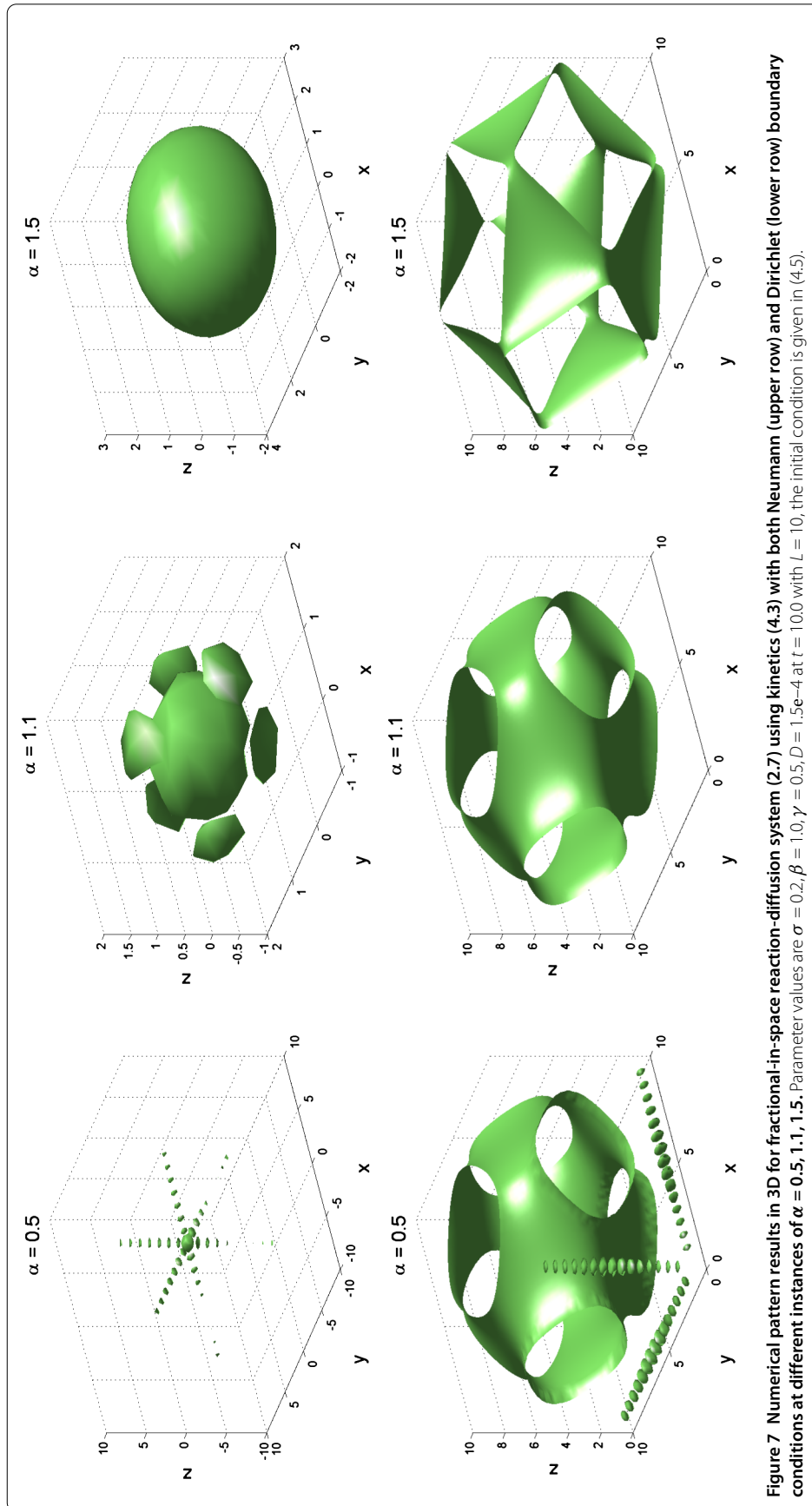


Figure 7 Numerical pattern results in 3D for fractional-in-space reaction-diffusion system (2.7) using kinetics (4.3) with both Neumann (upper row) and Dirichlet (lower row) boundary conditions at different instances of $\alpha = 0.5, 1.1, 1.5$. Parameter values are $\sigma = 0.2, \beta = 1.0, \gamma = 0.5, D = 1.5e-4$ at $t = 10.0$ with $L = 10$, the initial condition is given in (4.5).

cretization, we employ a fractional exponential integrator whose formulation is based on fourth order exponential time differencing to advance the resulting coupled system of ordinary differential equations in time. Two notable examples of reaction-diffusion systems taken from the literature are considered and formulated in space-fractional form. Our simulation results for the chosen examples show that pattern formations in the subdiffusive ($0 < \alpha < 1$) and superdiffusive ($1 < \alpha < 2$) scenarios are practically the same case as with the standard reaction-diffusion problems. The dynamic richness of our numerical techniques is explored in two and three space dimensions. The methodology in this research can be extended to solve multi-components integer- and non-integer-order systems.

Competing interests

The authors declare that there is no conflict of interests regarding the publication of this paper.

Authors' contributions

All authors read and approved the final manuscript.

Publisher's Note

Springer Nature remains neutral with regard to jurisdictional claims in published maps and institutional affiliations.

Received: 6 April 2017 Accepted: 19 July 2017 Published online: 03 August 2017

References

- Podlubny, I: Fractional Differential Equations. Academic Press, San Diego (1999)
- Podlubny, I, Chechkin, A, Skovranek, T, Chen, YQ, Jara, BB: Matrix approach to discrete fractional calculus II: partial fractional differential equations. *J. Comput. Phys.* **228**, 3137-3153 (2009)
- Gorenflo, R, Luchko, Y, Mainardi, F: Wright function as scale-invariant solutions of the diffusion-wave equation. *J. Comput. Appl. Math.* **118**, 175-191 (2000)
- Guo, B, Pu, X, Huang, F: Fractional Partial Differential Equations and Their Numerical Solutions. World Scientific, Singapore (2011)
- Gómex-Aguilar, JF, López-López, MG, Alvarando-Martínez, VM, Reyes-Reyes, J, Adam-Medina, M: Modeling diffusive transport with a fractional derivative without singular kernel. *Phys. A, Stat. Mech. Appl.* **447**, 467-481 (2016)
- Gómez-Aguilar, JF, Escobar-Jiménez, RF, Olivares-Peregrino, VH, Benavides-Cruz, M, Calderón-Ramón, C: Nonlocal electrical diffusion equation. *Int. J. Mod. Phys. C* **27**, 1650007 (2016)
- Gómex-Aguilar, JF, Miranda-Hernández, M, López-López, MG, Alvarando-Martínez, VM, Baleanu, D: Modeling and simulation of the fractional space-time diffusion equation. *Commun. Nonlinear Sci. Numer. Simul.* **30**, 115-127 (2016)
- Gómez-Aguilar, JF: Space-time fractional diffusion equation using a derivative with nonsingular and regular kernel. *Phys. A, Stat. Mech. Appl.* **465**, 562-572 (2017)
- Zhou, Y: Basic Theory of Fractional Differential Equations. World Scientific, New Jersey (2014)
- Ilic, M, Liu, F, Turner, I, Anh, V: Numerical approximation of fractional-in-space diffusion equation, I. *Fract. Calc. Appl. Anal.* **8**, 323-341 (2005)
- Kilbas, AA, Srivastava, HM, Trujillo, JJ: Theory and Applications of Fractional Differential Equations. Elsevier, New York (2006)
- Murray, JD: Mathematical Biology II: Spatial Models and Biomedical Applications. Springer, Berlin (2003)
- Owolabi, KM, Patidar, KC: Numerical simulations of multicomponent ecological models with adaptive methods. *Theor. Biol. Med. Model.* **13**, 1 (2016). doi:10.1186/s12976-016-0027-4
- Owolabi, KM: Mathematical analysis and numerical simulation of patterns in fractional and classical reaction-diffusion systems. *Chaos Solitons Fractals* **93**, 89-98 (2016)
- Henry, D: Geometric Theory of Semilinear Parabolic Equations. Springer, Berlin (1981)
- Hollis, SL, Martin, RH, Pierre, M: Global existence and boundedness in reaction-diffusion systems. *SIAM J. Math. Anal.* **18**, 744-761 (1987)
- Henry, BI, Wearne, SL: Fractional reaction-diffusion. *Physica A* **276**, 448-455 (2000)
- Henry, BI, Wearne, SL: Existence of Turing instabilities in a two-species fractional reaction-diffusion system. *SIAM J. Appl. Math.* **62**, 870-887 (2002)
- Pindza, E, Owolabi, KM: Fourier spectral method for higher order space fractional reaction-diffusion equations. *Commun. Nonlinear Sci. Numer. Simul.* **40**, 112-128 (2016). doi:10.1016/j.cnsns.2016.04.020
- Zeng, F, Li, C, Liu, F, Turner, I: Numerical algorithms for time-fractional subdiffusion equation with second-order accuracy. *SIAM J. Sci. Comput.* **37**, A55-A78 (2015)
- Zheng, M, Liu, F, Turner, I, Anh, V: A novel high order space-time spectral method for the time fractional Fokker-Planck equation. *SIAM J. Sci. Comput.* **37**, A701-A724 (2015)
- Zeng, F, Liu, F, Li, C, Burrage, K, Turner, I, Anh, V: A Crank-Nicolson ADI spectral method for a two-dimensional Riesz space fractional nonlinear reaction-diffusion equation. *SIAM J. Numer. Anal.* **52**, 2599-2622 (2014)
- Meerschaert, MM, Mortensen, J, Wheatcraft, SW: Fractional vector calculus for fractional advection-dispersion. *Physica A* **367**, 181-190 (2006)
- Liu, F, Anh, V, Turner, I: Numerical solution of the space fractional Fokker-Planck equation. *J. Comput. Appl. Math.* **166**, 209-219 (2004)

25. Liu, F, Anh, V, Turner, I, Zhuang, P: Numerical simulation for solute transport in fractal porous media. *ANZIAM J.* **45**, 461-473 (2004)
26. Ortigueira, MD: *Fractional Calculus for Scientists and Engineers*. Springer, New York (2011)
27. Atangana, A: On the stability and convergence of the time-fractional variable order telegraph equation. *J. Comput. Phys.* **293**, 104-114 (2015)
28. Meerschaert, MM, Tadjeran, C: Finite difference approximations for two-sided space-fractional partial differential equations. *Appl. Numer. Math.* **56**, 80-90 (2006)
29. Hanert, E: A comparison of three Eulerian numerical methods for fractional-order transport models. *Environ. Fluid Mech.* **10**, 7-20 (2010). doi:10.1007/s10652-009-9145-4
30. Hanert, E: On the numerical solution of space-time fractional diffusion models. *Comput. Fluids* **46**, 33-39 (2011). doi:10.1016/j.compfluid.2010.08.010
31. Roop, J: Computational aspects of FEM approximations of fractional advection dispersion equations on bounded domains on \mathbb{R}^2 . *J. Comput. Appl. Math.* **193**, 243-268 (2005)
32. Bueno-Orovio, A, Kay, D, Burrage, K: Fourier spectral methods for fractional-in-space reaction-diffusion equations. *BIT Numer. Math.* **54**, 937-954 (2014)
33. Khader, MM: On the numerical solutions for the fractional diffusion equation. *Commun. Nonlinear Sci. Numer. Simul.* **16**, 2535-2542 (2010)
34. Li, X, Xu, C: Existence and uniqueness of the weak solution of the space-time fractional diffusion equation and a spectral method approximation. *Commun. Comput. Phys.* **8**, 1016-1051 (2010)
35. Owolabi, KM, Patidar, KC: Existence and permanence in a diffusive KiSS model with robust numerical simulations. *Int. J. Differ. Equ.* **2015**, 485860 (2015). doi:10.1155/2015/485860
36. Krogstad, S: Generalized integrating factor methods for stiff PDEs. *J. Comput. Phys.* **203**, 72-88 (2005)
37. Owolabi, KM: Numerical solution of diffusive HBV model in a fractional medium. *SpringerPlus* **5**, 1643 (2016). doi:10.1186/s40064-016-3295-x
38. Cox, SM, Matthews, PC: Exponential time differencing for stiff systems. *J. Comput. Phys.* **176**, 430-455 (2002)
39. Kassam, AK, Trefethen, LN: Fourth-order time stepping for stiff PDEs. *SIAM J. Sci. Comput.* **26**, 1214-1233 (2005)
40. Du, Q, Zhu, W: Analysis and applications of the exponential time differencing schemes and their contour integration modifications. *BIT Numer. Math.* **45**, 307-328 (2005)
41. Owolabi, KM, Patidar, KC: Higher-order time-stepping methods for time-dependent reaction-diffusion equations arising in biology. *Appl. Math. Comput.* **240**, 30-50 (2014). doi:10.1016/j.amc.2014.04.055
42. Owolabi, KM, Patidar, KC: Numerical solution of singular patterns in one-dimensional Gray-Scott-like models. *Int. J. Nonlinear Sci. Numer. Simul.* **15**, 437-462 (2014). doi:10.1515/ijnsns-2013-0124
43. Owolabi, KM, Patidar, KC: Effect of spatial configuration of an extended nonlinear Kierstead-Slobodkin reaction-transport model with adaptive numerical scheme. *SpringerPlus* **5**, 303 (2016). doi:10.1186/s40064-016-1941-y
44. Beylkin, G, Keiser, JM, Vozovoi, L: A new class of time discretization schemes for the solution of nonlinear PDEs. *J. Comput. Phys.* **147**, 362-387 (1998)
45. Du, Q, Zhu, W: Stability analysis and applications of the exponential time differencing schemes. *J. Comput. Math.* **22**, 200-209 (2004)
46. Mott, DR, Oran, ES, van Leer, B: A quasi-steady-state solver for the stiff ordinary differential equations of reaction kinetics. *J. Comput. Phys.* **164**, 407-468 (2002)
47. Yang, Q, Turner, I, Liu, F, Ilić, M: Novel numerical methods for solving the time-space fractional diffusion equation in 2D. *SIAM J. Sci. Comput.* **33**, 1159-1180 (2011)
48. Guo, HJ, Chen, XX: Existence and global attractivity of positive periodic solution for a Volterra model with mutual interference and Beddington-DeAngelis functional response. *Appl. Math. Comput.* **217**, 5830-5837 (2011)
49. Haque, M: A detailed study of the Beddington-DeAngelis predator-prey model. *Math. Biosci.* **234**, 1-16 (2011)
50. Li, HY, Takeuchi, Y: Dynamics of the density dependent predator-prey system with Beddington-DeAngelis functional response. *J. Math. Anal. Appl.* **374**, 644-654 (2011)
51. Xue, L: Pattern formation in a predator-prey model with spatial effect. *Physica A* **391**, 5987-5996 (2012)
52. Garvie, M: Finite-difference schemes for reaction-diffusion equations modeling predator-prey interactions in MATLAB. *Bull. Math. Biol.* **69**, 931-956 (2007)
53. Garvie, M, Trenchea, C: Spatiotemporal dynamics of two generic predator-prey models. *J. Biol. Dyn.* **4**, 559-570 (2010)
54. Owolabi, KM: Robust and adaptive techniques for numerical simulation of nonlinear partial differential equations of fractional order. *Commun. Nonlinear Sci. Numer. Simul.* **44**, 304-317 (2016). doi:10.1016/j.cnsns.2016.04.021
55. Owolabi, KM, Atangana, A: Numerical solution of fractional-in-space nonlinear Schrödinger equation with the Riesz fractional derivative. *Eur. Phys. J. Plus* **131**, 335 (2016). doi:10.1140/epjp/i2016-16335-8
56. Owolabi, KM: Mathematical study of two-variable systems with adaptive numerical methods. *Numer. Anal. Appl.* **9**, 218-230 (2016). doi:10.1134/S1995423916030046